The effect of spatial light modulator (SLM) dependent dispersion on spatial beam shaping

Dirk-Mathys Spangenberg[a], Angela Dudley[b], Pieter Neethling[a], Andrew Forbes[b] and Erich Rohwer[a]

[a]Stellenbosch University, Private Bag X1, Matieland 7602, South Africa
[b]CSIR National Laser Centre, PO Box 395, Pretoria 0001, South Africa

ABSTRACT

SLMs used for spatial modulation of lasers are often used in conjunction with very narrow bandwidth laser light where diffractive dispersion could be approximated as a constant. It is known that diffractive dispersion is inversely proportional to wavelength and this effect can be compensated for depending on the optical set-up. SLMs use birefringent liquid crystal (LC) pixels each with an adjustable refractive index at a specific polarization. The range of the adjustable refractive index is wavelength dependent. This adds an additional SLM dependent dispersion. Note that we distinguish between diffractive dispersion and SLM dependent dispersion. SLMs are therefore calibrated in order to have linearly adjustable phase retardation of light incident on the pixels between zero and two pi for a specific wavelength. It is therefore unavoidable when using the same SLM, to do beam shaping of a source which emits multiple wavelengths or a wide bandwidth, that the device will not modulate all wavelengths between zero and two pi. We numerically and experimentally investigate the effect of SLM dependent dispersion on spatial modulation of light incident on a 2D SLM. We further discuss why it is possible to modulate multiple wavelengths between zero and two pi despite SLM dependent dispersion.

Keywords: spatial light modulator (SLM), dispersion, compensation, ultrashort pulse, spatial beam shaping

1. INTRODUCTION

The Fourier optical (FO) transform is a well known and documented phenomenon.[1] Programmable wave front shaping devices such as the 2D SLM makes generation and investigation of specific light fields possible,[2,3] Among others this device is used to study beams carrying orbital angular momentum (OAM).[4,5] It is common practice to apply a blazed grating to whichever pattern is loaded on the SLM in order to separate the light which cannot be altered, due to physically limiting artifacts such as the spacing between pixels, and the light which can be altered. This causes the light field which one can alter to focus in a different position in the Fourier optical plane with respect to the light which cannot be altered. A spatial filter can then be used to remove the unwanted light.

Our initial intention was to develop a method to measure the optical path length difference through the SLM for different wavelengths of light by using an all digital method which is based on the current accepted method. Our methodology was to measure the SLM dispersion using a commonly accepted method and then repeating the measurements using two all digital methods for comparison. Instead we discovered how wave front functions can be generated which shift between zero and two pi for different wavelengths of light and we mathematically explain how this is possible.

In this text the author will use the one dimensional temporal Fourier relations to demonstrate the operations performed between the input and the angular spectrum which in essence can simply be extrapolated to the two dimensional plane and scaled with a constant factor to obtain the correct FO transforms.

This article is structured as follows: First we explain the difference between diffractive dispersion and SLM dependent dispersion, we then discuss the experiments that lead to the discovery that SLM dependent dispersion is naturally compensated for in terms of phase but not amplitude. We show our measurements and numerical simulations where we made the observation and then show that this is consistent with the mathematical model.

Further author information: (Send correspondence to D.S.)
D.S.: E-mail: dspan@sun.ac.za, Telephone: +27-21-8083391

2. DISPERSION

In optics dispersion comes in two basic flavours, temporal and spatial dispersion where the term refers to the spreading of the spectral components. Temporal dispersion is when a light of different wavelengths travels through a medium at different speeds due to the medium having different refractive indices for different wavelengths of light. This introduces a phase difference between the different wavelengths of the light thereby causing the different wavelengths to disperse as it propagates through the medium. Spatial dispersion occurs when light with different wavelengths is incident on some mask which causes light with different wavelengths to diffract at different angles causing the different wavelengths to disperse spatially.

In the 2D SLM both temporal and spatial dispersion is realised. Temporal dispersion is realised by each pixel of the 2D SLM and adjusts the wave front of light passing through it by no more than a few wavelengths. The combination of many pixels allows us to generate a mask which causes spatial dispersion to occur.

The refractive index of the LC cells of the SLM has a wavelength dependence. This means that light will travel a different number of wave fronts for a fixed setting of the SLM when passing through a LC pixel cell. We refer to this as SLM dependent dispersion.

Wave front functions are realised by the combined wave front exiting the array of pixels each attributing a difference in the phase of the light passing through it. It is therefore of importance to know the SLM dependent dispersion when using broad band pulsed laser sources such as femtosecond lasers and laser sources which allows for the selection of multiple wavelengths such as super continuum sources with acousto optic modulators (AOM) for output coupling.

3. MEASURING THE SLM DISPERSION USING A PHYSICAL MASK

The SLM is connected to a video output of the computer and translates different grey level intensities, written to the SLM as a monitor, to voltage levels. The applied voltage level across the end faces of a single nematic crystal causes the elongated crystals to try to align with the electric field by tilting in the plane formed by the z-axis and the extraordinary axis. The extraordinary axis lies perpendicular to the z axis and along the elongation of the nematic crystals. This tilting of the nematic crystals results in a change in the refractive index along the extraordinary axis. If the SLM is only illuminated with light polarized along this axis then one can adjust the optical path length of the light through each nematic crystal pixel. This is done simply by displaying a grey scale mask on the SLM with a bit depth of typically 256 levels. Each grey scale level can be calibrated to represent a specific voltage level such that the refractive index and therefore the path length through the pixels of the SLM scales linearly with the grey level setting to give a path length difference between zero and two pi.

During the calibration of the SLM one essentially determines the relationship between voltage levels sent to the SLM and the resultant phase difference. The standard method of calibration is based on a phase shift introduced to one of two equidistant point sources and can be explained as follows:

Given two equally spaced, $\pm x_0$, delta functions where the phase of one delta function can be adjusted by ϕ,

$$f(x) \quad = \quad e^{j\phi}\delta(x - x_0) + \delta(x + x_0).$$

The Fourier transform of $f(x)$ is,

$$F(X) \quad = \quad 2e^{j\frac{\phi}{2}}\cos\left(Xx_0 - \frac{\phi}{2}\right). \tag{1}$$

Rewritten to show the shift in the spectral domain explicitly $F(X)$ becomes

$$F(X) \quad = \quad 2e^{j\frac{\phi}{2}}\cos(Xx_0) \circledast \delta\left(X - \frac{\phi}{2x_0}\right).$$

The finite size of the input mask can simply be accounted for by a function $u(t) = \text{rect}(t/a)$ such that,

$$u(x) \circledast f(x) \quad = \quad \text{rect}\left(\frac{x}{a}\right) \circledast f(x) \tag{2}$$

$$\underset{\Leftrightarrow}{\Im} \quad \text{sinc}\left(\frac{Xa}{2}\right) \times F(X) \tag{3}$$

$$= \quad \text{sinc}\left(\frac{Xa}{2}\right) \times \left[2e^{j\frac{\phi}{2}}\cos\left(Xx_0 - \frac{\phi}{2}\right)\right]. \tag{4}$$

It is clear from Eq. 4 that the finite size of the holes in the mask will not affect the phase shift in the FO plane only the intensity distribution.

The calibration is done by placing a mask with two holes, referred to as the physical mask method, in front of the SLM such that the light passing through each hole falls on one half of the SLM, see Fig. 1. The grey level of one half of the SLM is set to a fixed value while the other is kept at zero. The shift in the interference pattern, described by Eq. 1, is measured directly on the resultant pattern which forms in the FO plane. This phase shift is always measured with respect to the pattern formed when the grey level of both halves of the SLM is kept at zero. The procedure is repeated for all possible pixel level settings and an inverse lookup table is calculated and stored on the SLM as a gamma curve.
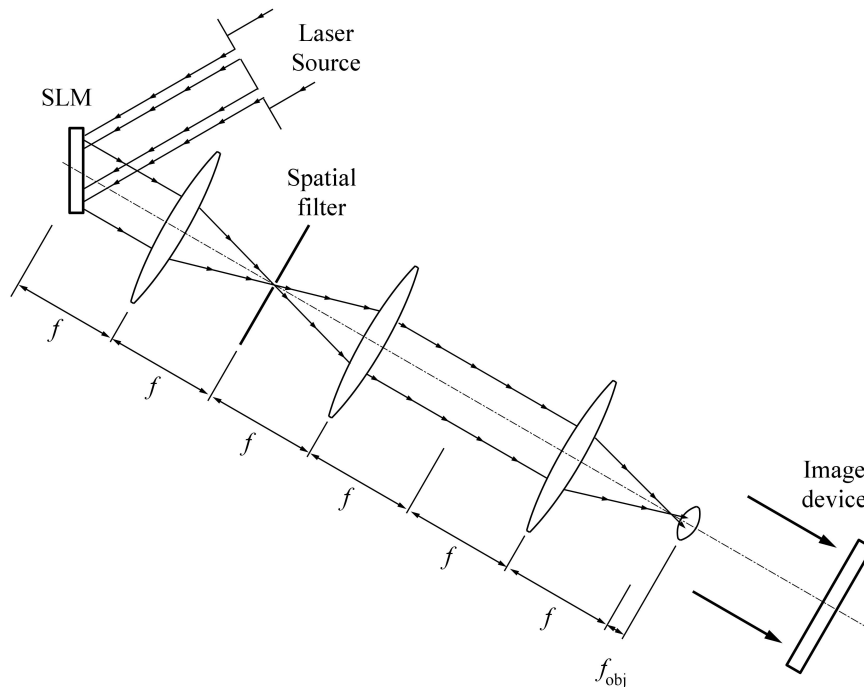

Figure 1. Schematic of the physical two spot mask optical setup. Scale and angles are exaggerated.

Theoretically to calculate the gamma curve, the measured data points are interpolated to give us a function,

$$f(p) \quad = \quad \phi,$$

the inverse function is then used do determine a discrete set of values for p such that the set of p_n gives us a corresponding set of ϕ values which scales linearly between zero and 2π. Thus for

$$f^{-1}\left(\frac{2\pi n}{256}\right) \quad = \quad \{p_n\}, \text{ where } n \in \mathbb{N}, 0 \le n < 256,$$

the set $\{p_n\}$ then represents the inverse function and therefore the calibration set and thus we have

$$f\left(p_n\right) \;\; = \;\; \frac{2\pi}{n} + \phi_k, \tag{5}$$

at the calibration wavelength. It has to be noted that we are only interested in the difference in wavelength change between the pixels in the device and not the absolute phase and therefore we can simplify Eq. 5 to

$$f\left(p_n\right) \;\; = \;\; \frac{2\pi}{n}. \tag{6}$$

We used the physical mask method to calibrate our SLM such that it had a linear zero to two pi response for pixel value settings between 0 and 255 at a wavelength of 715 nm, using software supplied by the manufacturer to calculate the gamma curve. With the phase shift corrected to be linear for 715 nm and measuring the phase shift using the same calibration set we found that the resultant measured curves were also linear from 475 nm to 775 nm with only the gradient changing, see examples in Figures 2(a),2(b), 2(c) and 2(d).
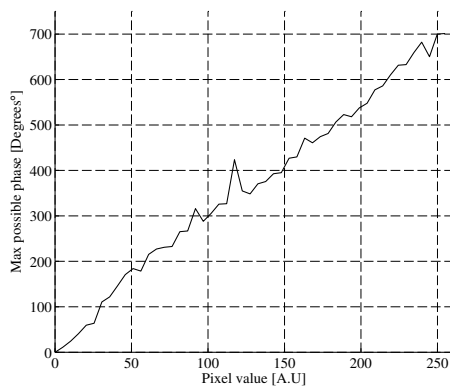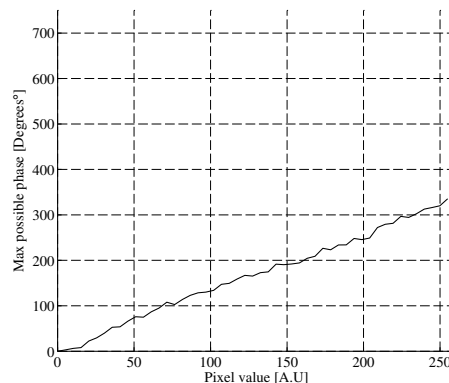

(a) Measured phase shift at 475 nm of the SLM when calibrated for 710 nm.
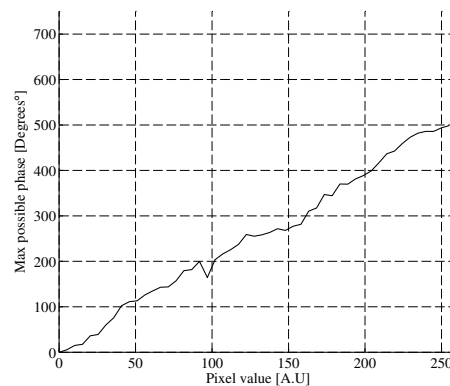
(b) Measured phase shift at 550 nm of the SLM when calibrated for 710 nm.
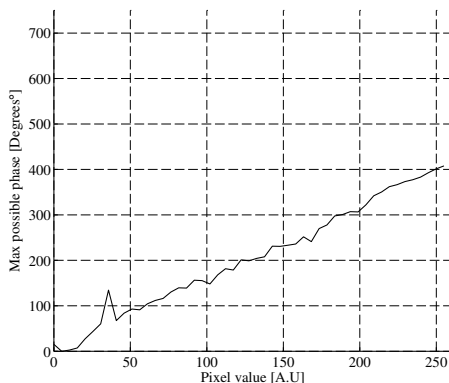
(c) Measured phase shift at 650 nm of the SLM when calibrated for 710 nm.

(d) Measured phase shift at 775 nm of the SLM when calibrated for 710 nm.

Figure 2. Measured phase shift at 475 nm, 550 nm, 650 nm and 775 nm with SLM calibrated for 170 nm.

From these measurements we make the following approximation within the range of wavelengths $4\,75 - 775$ nm. If we measure the change in optical path length introduced for a specific wavelength, λ_c, for all possible grey level settings, v, such that we have the measured function $\Delta\lambda\left(v,\lambda_c\right)$, then for any other wavelength we can determine a constant such that,

$$k_d\left(\lambda\right) \;\; = \;\; \frac{\Delta\lambda\left(v,\lambda\right)}{\Delta\lambda\left(v,\lambda_c\right)}, \tag{7}$$

where the function $k_d(\lambda)$ is independent of v and thus

$$\Delta\lambda(\lambda) \quad \propto \quad \Delta\lambda(\lambda_c).$$

According to the relation in Eq. 7 we need only use two reference points to calculate a $\Delta\lambda$ for λ_c and the wavelength for which we want to find k_d by calculating $k_d = \frac{\Delta\lambda}{\Delta\lambda_c}$. We used 50 data points, chosen to have intensities which are equally spaced between zero and 255, in the measurements depicted by our graphs. Thus our sample set size is $N = 50$, giving a statistically better average. Since the change in optical path length for grey level settings between 0 and 255 is linear we could determine k_d simply by calculating the gradient of the grey level setting with respect to the shift in wavelength. Thus we can rewrite Eq. 2 as,

$$f(x) \quad = \quad \text{rect}\left(\frac{x}{a}\right) \circledast \left[e^{jk_d\phi}\delta(x - x_0) + \delta(x + x_0)\right], \tag{8}$$

and its Fourier transform,

$$F(X) \quad = \quad \text{sinc}\left(\frac{Xa}{2}\right) \times \left[2e^{j\frac{k_d\phi}{2}}\cos\left(Xx_0 - \frac{k_d\phi}{2}\right)\right]. \tag{9}$$

Using Eq. 9 we can determine k_d. This was done for wavelengths from $475\,\text{nm}$ to $775\,\text{nm}$ in incremental steps of $25\,\text{nm}$, see Fig. 3.
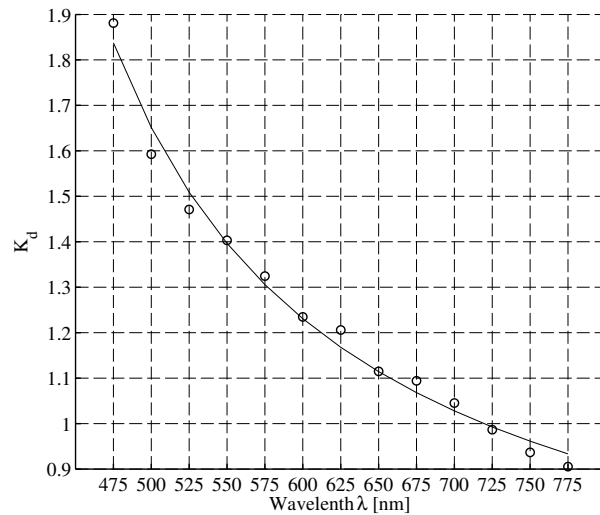

Figure 3. k_d measured at different wavelengths. Measured values indicated by circles and $\frac{1}{x}$ function fit in solid.

These results, based on the accepted calibration method, shows that there is a relationship between the wavelength and the introduced path difference by the SLM. Further the results indicate that the optical path length through a crystal pixel unit at a fixed crystal orientation will scale linearly with wavelength.

4. SLM DISPERSION MEASUREMENT USING DIGITAL MASKS

We used two digital masks in the all digital part of the experiment. The first, which we will refer to as the digital two spot mask, is a digital representation of the physical two spot mask and the second is a double annular ring mask which results in a petal beam in the FO plane. Blazed gratings of different periodicity and angles are applied, to minimise order overlap, to the wanted pattern and the unwanted background causing these to focus at different positions in the FO plane which allows us to filter out the background with a spatial filter, see Fig. 4.
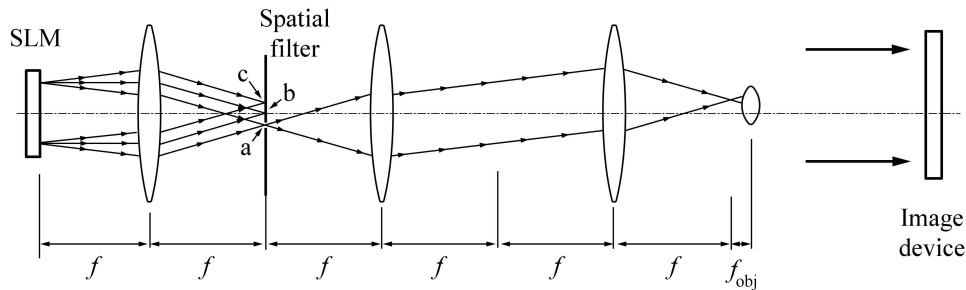
Figure 4. Schematic of the optical setup used in the experiment. Illustrated in (a) are rays originating from the two spots due to the applied blazed grating, (b) rays not affected by the applied SLM mask and (c) the rays originating from the background with a grating in the opposite direction.

4.1 Digital two spot mask

In the digital two spot mask, see Fig. 5, light incident on the two spots will propagate in a direction determined by the applied blazed grating. Measurements using the digital two spot mask system is done in the same way as the physical mask method, only now measurements are made in the position of the first diffractive order where light from the applied blazed grating come to a focus. The measured shift in the pattern can be used to calculate the difference in phase between the two spots in the same way that it is done for the physical mask method through the relation given by Eq. 9.
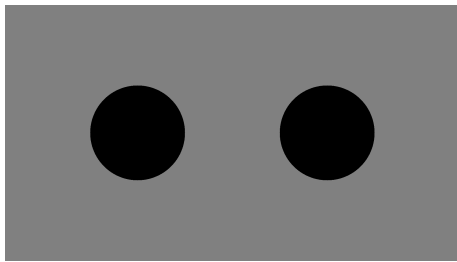
(a) Qualitative illustration of the digital two spot mask without the blazed grating.
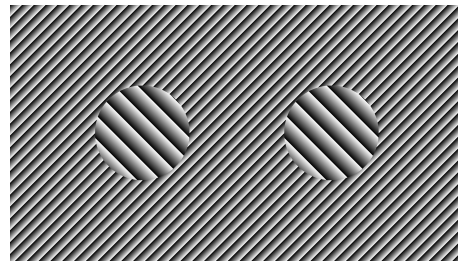
(b) Qualitative illustration of the digital two spot mask with the applied blazed grating.

Figure 5. Qualitative illustration of the digital two spot mask with and with out the blazed grating.

In the two spot mask experiment we used two masks, one with no phase difference between the two spots and one with a setting of 0.5 which according to Eq. 9 must correspond to $k_d\pi$. We used the same two masks measuring the phase difference introduced within a range of wavelengths from 475 nm to 800 nm, see Fig. 6.
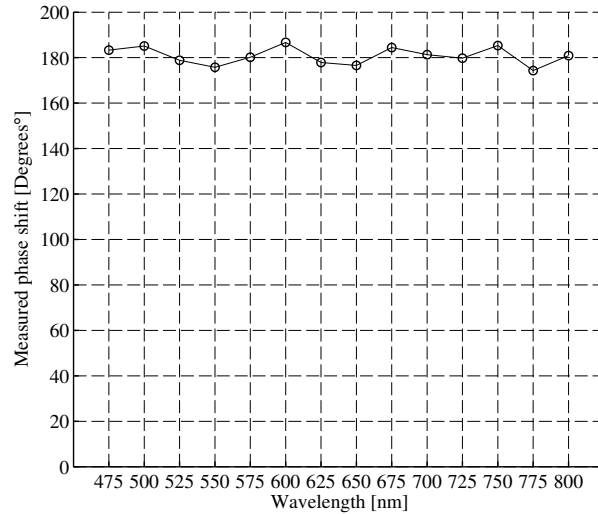
Figure 6. Resultant phase shift when the starting phase level for pixels of the one spot is set to 128 before the blazed grating is added.

4.2 Annular ring mask

The double annular ring mask consist of two annular rings each with a varying phase on the radial axis of $2\pi n$. These rings are thin and can be approximated as ring slit sources. Each ring will result in a Bessel pattern in the FO plane with azimuthally varying phase which when superimposed will interfere constructively and destructively resulting in a petal pattern. The angle of this pattern is dependent on the relative phase difference between the inner and outer rings.
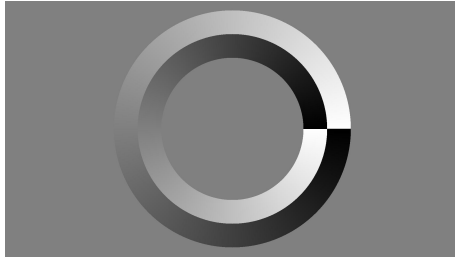
(a) Qualitative illustration of the digital petal mask without the blazed grating.
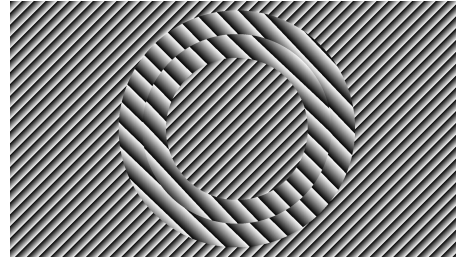
(b) Qualitative illustration of the digital petal mask with the blazed grating.

Figure 7. Qualitative illustration of the digital petal mask with and without the blazed grating.

One can investigate the relative phase shift between two masks by noting the angle between resultant petals. This is done by determining the Fourier transform of the input function,

$$f(r,\theta) = \begin{cases} e^{il\theta} & \text{for } r_1 - \frac{\Delta}{2} \leq r \leq r_1 + \frac{\Delta}{2} \\ e^{-i[l\theta+\delta]} & \text{for } r_2 - \frac{\Delta}{2} \leq r \leq r_2 + \frac{\Delta}{2} \\ 0 & \text{elsewhere}, \end{cases} \tag{10}$$

of which the Fourier transform is,

$$F(R,\phi) \quad \propto \quad J_l(k_{1r}R)\,e^{i[l\phi+\delta]}e^{ik_{1z}f} + J_{-l}(k_{2r}R)\,e^{-il\phi}e^{ik_{2z}f}. \tag{11}$$

If the rings are approximated as thin and on top of each other one can write the intensity as

$$|F(R,\theta)|^2 \quad \approx \quad J_l(k_r R)\left[1 + (-1)^l \cos(2l\phi + \delta)\right]. \tag{12}$$

One can calculate the phase δ by measuring the change in the rotation angle of the petal pattern when a fixed pixel offset level is added to one of the rings.

In the two annular ring experiment we used an annular ring mask with the inner ring shifted by adding a constant value of 32 to the inner ring which corresponds to a rotation of the inner ring by $\frac{\pi}{4}$ after modulating the pattern by 255. We measured the change in the phase shift in the resultant pattern in the FO plane by using the same mask for a range of wavelengths from 475 nm to 800 nm, see Fig. 8.
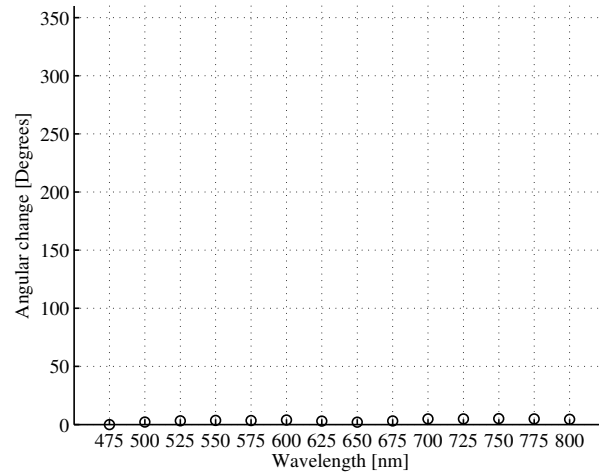

Figure 8. Resultant phase shift when $\frac{\pi}{4}$ phase is applied to the inner ring of the double annular ring pattern.

Fig. 8 shows no change, within the range of measurement error, in phase for the different wavelengths.

To verify the linearity of the phase shift of the pattern rotation in the FO plane when a phase shift is introduced to the inner annular ring, we measured the phase at the FO plane with respect to all possible SLM pixel values between $0 - 255$. The measurement in Fig. 9 was taken at 525 nm where the measured k_d value is 1.45, taking 10 samples for each level.
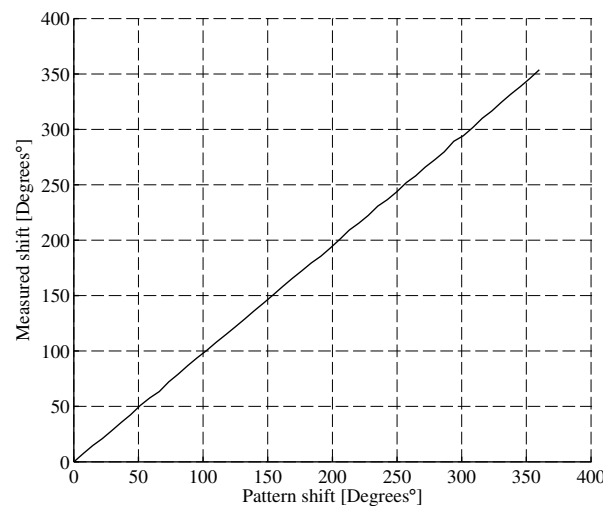

Figure 9. Measurement of phase shift in the FO plane with respect to phase shift introduced to the inner annular ring at the input ring mask pattern.

It is clear from Fig. 9 that the shift introduced by the phase mask is $0 - 2\pi$ despite a non unity value for k_d.

4.3 Discussion

These results contradict what we expected to find. We are certain that there is a phase shift introduced by the SLM which is dependent on wavelength, yet the results from our experiment shows that the interference patterns behaves as if modulated perfectly between zero and 2π. These results can be numerically reproduced, therefore the explanation must be inherent in the mathematics.

5. PERIODIC MODULATED DECOMPOSITION OF A LINEAR PHASE GRADIENT

During our initial experiments we noticed some other effects which occurred in higher diffraction orders, these were effectively filtered out by the spatial filter in our setup. In order to understand what we observed, we also investigated these effects by removing the spatial filter.

First we noticed that the different orders which stems from a non unity k_d value are multiples of the order of our input function. This is plainly visible for petal functions as is illustrated in Fig. 10(a).
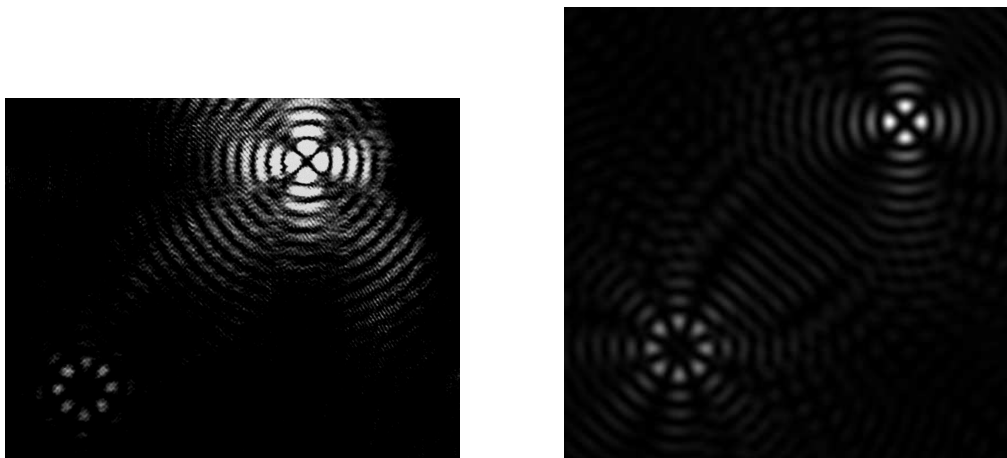
(a) Measured first and second order of an input beam with azimuthally varying phase of $l = (-2, 2)$.

(b) Numerically calculated first and second order of an input beam with azimuthally varying phase of $l = (-2, 2)$.

Figure 10. First and second order of an input beam with azimuthally varying phase of $l = (-2, 2)$ both measured and numerically calculated.

We also noticed that if we added a phase difference between the two annular rings or the two spots on the input mask, the resultant shift of the pattern would be a multiple of the diffraction order of our applied grating. These observations which appear to be linked to the diffraction orders of the applied grating lead us to investigate the non-ideal blazed grating and therefore the effect of a modulation function on a linear phase gradient in the Fourier optical plane. The mathematical analysis follows below.

If one considers a continuous linear phase,

$$g(x) \quad = \quad e^{jkx} \tag{13}$$

where

$$k \quad = \quad \text{The gradient,}$$

then by defining a new parameter w such that the phase difference for each $\Delta\phi = 2\pi$ is $\Delta x = w$ and substituting these into Eq. 13 one can write,

$$g(x) \quad = \quad e^{j\frac{2\pi x}{w}}. \tag{14}$$

When a diffractive element such as a blazed grating is used to realise a linear phase gradient there is a wavelength dependence which has to be accounted for. It is known that the pitch for a blazed grating will be constant and therefore the gradient can be written to account for the different gradients seen by different wavelengths by adding a scaling constant k_d to Eq. 14,

$$k = \frac{\Delta\phi}{\Delta x} \tag{15}$$

$$= \frac{2\pi k_d}{w}, \tag{16}$$

where w now represents the pitch of the blazed grating. The blazed grating can now be accurately represented by the modulated function in the temporal domain given by,

$$g(x) = e^{\frac{2\pi k_d}{w}x} \times \text{rect}\left(\frac{2}{w}x\right) \circledast \sum_{n=-\infty}^{\infty} \delta(x - nw), \tag{17}$$

which can be simplified to, see Section A for proofs,

$$g(x) = \sum_{n=-\infty}^{\infty} \text{sinc}\left(\pi[n - k_d]\right) e^{j\frac{2\pi n}{w}x}. \tag{18}$$

Written in a more general form by making w the subject of Eq. 16

$$w = \frac{2\pi k_d}{k}, \tag{19}$$

and substituting it into Eq. 18 one finds,

$$g(x) = \sum_{n=-\infty}^{\infty} \text{sinc}\left(\pi[n - k_d]\right) e^{j\frac{kn}{k_d}x}. \tag{20}$$

Thus one can write a general expression for the modulus decomposition of a linear phase as

$$\text{mod}\left(e^{jkx}, k_d\right) = \sum_{n=-\infty}^{\infty} \text{sinc}\left(\pi[n - k_d]\right) e^{j\frac{kn}{k_d}x}. \tag{21}$$

It is clear from Eq. 21 that if one modulates any linear gradient input function where there is a linear gradient scaling constant k_d multiplied with the gradient, then these would cancel out and the resultant patterns would only represent the scaling factor in their intensities.

Now it remains to show that the modulation would account for the observed effects in both the digital two spot mask and the annular ring mask experiments.

6. LINEAR GRADIENTS IN THE 2 SPOT MASK

The equation for the digital two spot mask can be written as the expression for a two spot mask multiplied by the expression for a blazed grating. We have already shown that the blazed grating will decompose into different blazed grating orders such that k_d is not present in the phase shift of the resultant pattern, see Eq. 18, and we know that the two spot mask would simply be the multiplication of the two spot mask function with the applied blazed grating function,

$$f(x) = \text{rect}\left(\frac{x}{a}\right) \circledast \left[e^{jk_d\phi}\delta(x - x_0) + \delta(x + x_0)\right]. \tag{22}$$

It is not apparent when looking at Eq. 22 how the modulus operation would have an effect, only when rewriting the equation as,

$$f(x) = \text{rect}\left(\frac{x}{a}\right) \circledast \left[e^{j\frac{k_d\phi}{2}} \left[\delta(x - x_0) + \delta(x + x_0) \right] \times e^{j\frac{k_d\phi}{2x_0}x} \right], \tag{23}$$

can it be seen that there is a hidden linear gradient component which of course we can decompose using the modulus decomposition function given by Eq. 21.

The resultant decomposition of the linear gradient component, for $k = \frac{k_d\phi}{2x_0}$, is given by,

$$\text{mod}\left(e^{j\frac{k_d\phi}{2x_0}x}, k_d \right) = \sum_{m=-\infty}^{\infty} \text{sinc}\left(\pi[m - k_d] \right) e^{j\frac{m\phi}{2x_0}x}, \tag{24}$$

from which it is apparent that if the orders are separated into different positions then we cannot measure k_d.

The way in which the orders becomes separated into different positions is actuated through multiplication by the grating equation which means a convolution in the spectral domain such that we have,

$$f(x)g(x) = \text{rect}\left(\frac{x}{a}\right) \circledast \left[e^{j\frac{k_d\phi}{2}} \left[\delta(x - x_0) + \delta(x + x_0) \right] \times \left(\sum_{m=-\infty}^{\infty} \text{sinc}\left(\pi[m - k_d] \right) e^{j\frac{m\phi}{2x_0}x} \right) \times \right. \\ \left. \sum_{n=-\infty}^{\infty} \text{sinc}\left(\pi[n - k_d] \right) e^{j\frac{2\pi n}{w}x} \right], \tag{25}$$

which can be simplified because the function only exist where $m = n$ thus,

$$f(x)g(x) = \text{rect}\left(\frac{x}{a}\right) \circledast \left[e^{j\frac{k_d\phi}{2}} \left[\delta(x - x_0) + \delta(x + x_0) \right] \times \left(\sum_{n=-\infty}^{\infty} \text{sinc}\left(\pi[n - k_d] \right) e^{j\left[\frac{2\pi n}{w} + \frac{n\phi}{2x_0}\right]x} \right) \right]. \tag{26}$$

One can take Eq. 26 to the spectral domain to find

$$F(X) \circledast G(X) = \text{sinc}\left(\frac{Xa}{2}\right) \times \left(e^{j\frac{k_d\phi}{2}} 2\pi \cos(Xx_0) \circledast \left[\sum_{n=-\infty}^{\infty} \text{sinc}\left(\pi[n - k_d] \right) \delta\left(X - \left[\frac{2\pi n}{p} + \frac{n\phi}{2x_0} \right] \right) \right] \right), \tag{27}$$

from which we can clearly see that the factor k_d cannot be measured by measuring the shift at the orders and that the amount of shift will be scaled by the order number where we do the measurement. With the proof of how a two spot modulated function can be decomposed into a series of weighted linear spectral gradients we know that by applying the superposition principle one can construct any field from the sum of two spot functions of arbitrary size and position and therefore the modulation function would apply to any input function.

In conclusion we found that our experimental results can be explained by taking the modulus operation into account. It also indicates that when using the modulus operation in conjunction with a phase mask and a blazed grating which moves the beam off axis, the phase mask will behave as if the phase is perfectly calibrated between zero and two pi regardless of the SLM dependent dispersion constant k_d. The effect of the SLM dependent dispersion will be present in the form of an amplitude scaling of the intensity.

APPENDIX A. MATHEMATICAL PROOFS

Consider the temporal grating,

$$g(x) = e^{j\frac{2\pi k_d}{p}x} \text{rect}\left(\frac{2}{p}x\right) \circledast \sum_{n=-\infty}^{\infty} \delta(x - np).$$

Now we take the Fourier transform

$$
\begin{aligned}
G\left(X\right) &= 2\pi\delta\left(X - \frac{2\pi k_d}{p}\right) \circledast \operatorname{sinc}\left(X\frac{p}{2}\right) \times \sum_{n=-\infty}^{\infty} \delta\left(X - \frac{2\pi n}{p}\right) \\
&= 2\pi\operatorname{sinc}\left(\left[X - \frac{2\pi k_d}{p}\right]\frac{p}{2}\right) \times \sum_{n=-\infty}^{\infty} \delta\left(X - \frac{2\pi n}{p}\right) \\
&= 2\pi\sum_{n=-\infty}^{\infty} \operatorname{sinc}\left(\left[\frac{2\pi n}{p} - \frac{2\pi k_d}{p}\right]\frac{p}{2}\right)\delta\left(X - \frac{2\pi n}{p}\right) \\
&= 2\pi\sum_{n=-\infty}^{\infty} \operatorname{sinc}\left(\pi\left[n - k_d\right]\right)\delta\left(X - \frac{2\pi n}{p}\right).
\end{aligned}
$$

Taking the simplified spectral grating function back to the temporal domain we find,

$$
g\left(x\right) = \sum_{n=-\infty}^{\infty} \operatorname{sinc}\left(\pi\left[n - k_d\right]\right)e^{j\frac{2\pi n}{p}x}.
$$

ACKNOWLEDGMENTS

REFERENCES

1. J. W. Goodman, *Introduction to Fourier Optics*, Roberts & Company, 2005.
2. R. Vasilyeu, A. Dudley, N. Khilo, and A. Forbes, "Generating superpositions of higher-order bessel beams," *Optics Express* **17**, pp. 23389–23395, 2009.
3. I. A. Litvin, A. Dudley, F. S. Roux, and A. Forbes, "Azimuthal decomposition with digital holograms," *Optics Express* **20**, pp. 10996–11004, 2012.
4. A. Dudley, I. A. Litvin, and A. Forbes, "Quantitative measurement of the orbital angular momentum density of light," *Applied Optics* **51**, pp. 823–833, 2012.
5. A. Dudley and A. Forbes, "From stationary annular rings to rotating bessel beams," *Journal of the Optical Society of America A* **29**, pp. 567–573, 2012.